ORIGINAL ARTICLE

Complete genome sequence of *Photobacterium ganghwense* C2.2: A new polyhydroxyalkanoate production candidate

Irina Lascu[1] | Ioana Mereuță[1] | Iulia Chiciudean[1] | Hilde Hansen[2] | Sorin Marius Avramescu[3] | Ana-Maria Tănase[1] | Ileana Stoica[1]

[1]Department of Genetics, Faculty of Biology, University of Bucharest, Bucharest, Romania

[2]Department of Chemistry, Faculty of Science and Technology, UiT The Arctic University of Norway, Tromsø, Norway

[3]Department of Organic Chemistry, Biochemistry and Catalysis, Faculty of Chemistry, University of Bucharest, Bucharest, Romania

Correspondence
Iulia Chiciudean and Ana-Maria Tănase, Department of Genetics, Faculty of Biology, University of Bucharest, Bucharest, Romania.
Emails: iulia.chiciudean@bio.unibuc.ro; ana-maria.tanase@bio.unibuc.ro

Abstract

Polyhydroxyalkanoates (PHAs) are biodegradable bioplastics that can be manufactured sustainably and represent a promising green alternative to petrochemical-based plastics. Here, we describe the complete genome of a new marine PHA-producing bacterium—*Photobacterium ganghwense* (strain C2.2), which we have isolated from the Black Sea seashore. This new isolate is psychrotolerant and accumulates PHA when glycerol is provided as the main carbon source. Transmission electron microscopy, specific staining with Nile Red visualized via epifluorescence microscopy and gas chromatography analysis confirmed the accumulation of PHA. This is the only PHA-producing *Photobacterium* for which we now have a complete genome sequence, allowing us to investigate the pathways for PHA production and other secondary metabolite synthesis pathways. The de novo assembly genome, obtained using open-source tools, comprises two chromosomes (3.5, 2 Mbp) and a megaplasmid (202 kbp). We identify the entire PHA synthesis gene cluster that encodes a class I PHA synthase, a phasin, a 3-ketothiolase, and an acetoacetyl-CoA reductase. No conventional PHA depolymerase was identified in strain C2.2, but a putative lipase with extracellular amorphous PHA depolymerase activity was annotated, suggesting that C2.2 is unable to degrade intracellular PHA. A complete pathway for the conversion of glycerol to acetyl-CoA was annotated, in accordance with its ability to convert glycerol to PHA. Several secondary metabolite biosynthetic gene clusters and a low number of genes involved in antibiotic resistance and virulence were also identified, indicating the strain's suitability for biotechnological applications.

KEYWORDS
complete-genome, glycerol, marine bacteria, *Photobacterium*, polyhydroxyalkanoates

---

Irina Lascu and Ioana Mereuță have contributed equally to this work..

Iulia Chiciudean and Ana-Maria Tănase have jointly supervised this work.

---

1 | INTRODUCTION

The adverse effects plastic waste has on our biosphere (Chae & An, 2018; Eriksen et al., 2014; Sebille et al., 2015) demand a global need to implement plastic clean-up strategies and replace petrochemical-based plastics with biodegradable, bio-based polymers (Haward, 2018). Polyhydroxyalkanoates (PHAs) are a group of thermoplastic biopolyesters (Harding et al., 2007; Raza et al., 2018; Zhang et al., 2018) which are biodegradable and immunologically inert (Wang et al., 2014). The most common PHA is polyhydroxybutyrate (PHB), which can be produced by diverse bacteria (Inoue et al., 2016; Koller et al., 2011; Muhammadi et al., 2015; Sathiyanarayanan et al., 2017), which synthesize and store it as intracellular reserves of carbon and energy (Cavaillé et al., 2016; Keshavarz & Roy, 2010; Sedlacek et al., 2019; Slaninova et al., 2018). The most prevalent bacteria used in industrial bioplastic production are (1) *Cupriavidus necator* H16 (Yield10 Bioscience; CJ CheilJedang; Tianjin GreenBio Materials Co.; TianAn Biologic Materials Co.; Bio-On Srl.), (2) *Alcaligenes* sp. (Biomer; HB Industrial S.A.); and (3) genetically engineered *Escherichia coli* that received PHA synthesis genes from naturally PHA producing bacteria such as *C. necator* H16 (Patent no. US5480794A, former Metabolix), *Rhodospirillum rubrum* (Patent no. US5849894A, CJ CheilJedang Corp), or *Ralstonia eutropha* modified to express the synthase gene from *Pseudomonas fluorescens* GK-13 (Danimer Scientific; Noda et al., 2005). However, commercialization and production of bacterial PHA are constrained by its expensive substrates such as refined sugars, starch, or valuable plant oil (Koller & Marsalek, 2015), making its price twofold that of conventional, petroleum-based plastics (average cost of PHB was reported to be approx. 4.88 USD/kg; Raza et al., 2018).

To decrease the production costs, a PHA producing strain should be able to grow to high cell densities and accumulate large amounts of PHA at the account of inexpensive carbon resources such as glycerol (Gahlawat & Soni, 2017; Poblete-Castro et al., 2014), waste cooking oil (Sangkharak et al., 2020; Vastano et al., 2019), or other low-cost biomass (whey, starch, spent coffee grounds, wastewaters, wheat, and rice straw, lignin, etc.; Alcântara et al., 2020). As biodiesel production is increasing, the glycerol market has expanded rapidly, and using this by-product as a cheap substrate could be integrated into a circular economy approach (El-malek et al., 2020). In this context, we isolated a new strain of *Photobacterium ganghwense* that can convert glycerol to biodegradable polymers (PHA) in the form of poly-3-hydroxybutyrate (PHB).

The *Photobacterium* genus encompasses Gram-negative, facultative-anaerobic, and motile bacteria, which are widespread throughout marine environments where some species live symbiotically with marine animals (Urbanczyk et al., 2011). This genus is relatively new, with 22 of the 28 existing species described within the last 15 years (Labella et al., 2017; Machado & Gram, 2017). Although several draft genomes are available, complete genomes exist for only three species (*P. damselae*, *P. profundum*, and *P. gaetbulicola*). Neither one of them is documented as a PHA producer.

The biotechnological potential of this genus is yet to be explored and most studies have focused on individual members' pathogenicity toward animals and humans (Abushattal et al., 2020; Fumanal et al., 2020; Rivas et al., 2013; Romalde, 2002). Information regarding PHA production within the *Photobacterium* genus is scarce and, to our knowledge, only two species (*P. leiognathi* and *P. phosphoreum*) have been described to accumulate intracellular PHAs when provided with glycerol and peptone as carbon and nitrogen substrates (Boyandin et al., 2008). None of these PHA-producing *Photobacterium* has a complete genomic sequence publicly available.

In this study, we report the isolation of a new PHA-producing *Photobacterium ganghwense* (Park et al., 2006) strain (C2.2) and its complete genomic sequence, the first complete sequence available for this species. Furthermore, we present strain C2.2's PHA production phenotype, its genetic basis, and provide valuable insights into other predicted metabolic capacities, gene transfer, structural modifications, virulence, and antibiotic resistance.

2 | MATERIALS AND METHODS

2.1 | Bacterial isolation and PHA screening

A wet sand sample was collected in February 2018 from a Black Sea beach on the Romanian shoreline (location coordinates: 44.215993; 29.656308; marine water temperature 2°C, pH 7, salinity 17‰; Appendix Table A1). To detach the bacterial cells from sand particles, the sample was placed on a rotative incubator (150 rpm) in filter-sterilized marine water for 5 days at 20°C. After the detachment step, the aqueous phase was collected by centrifugation (6000 g, 5 min, 24°C), serially diluted up to 10^{-4} and spread (100 µl) on solid artificial seawater media (ASW) supplemented with 1 g/L yeast extract, 1 ml trace element solution, and 10 ml vitamin solution (ASW-Y media; Xiao & Jiao, 2011). Morphologically distinct colonies grown on ASW-Y media were selected and isolated. To screen for PHA-production the solid ASW media was supplemented with sterile glycerol (2% w/v) and Nile Red staining solution (0.25 mg/ml) immediately after autoclavation. Plates with glycerol and Nile Red for PHA screening were inoculated with the previously isolated bacterial strains and incubated in the dark for 14 days (20°C). The formation of fluorescent granules (PHA accumulation) was evaluated daily using wet mount slides and viewed through epifluorescence microscopy (Zeiss Axioplan, Carl Zeiss, Germany; FS00 filter (λ_{ex}: 545/±25 nm, λ_{em}: 560–710 nm).

2.2 | Bacterial strain identification

The bacterial strain was identified by 16S rRNA gene sequence similarity. The genomic DNA was extracted with the PureLink Genomic DNA Extraction kit (Invitrogen, #K1820), according to the manufacturer's instructions. DNA quantity and quality were evaluated by 0.8% agarose gel electrophoresis and Qubit dsDNA BR assay

kit (Life Technologies, #Q32850). 16S rRNA gene sequence was amplified with the universal primers 27F/1429R. The PCR product was purified and sequenced at Genetic Lab (http://www.geneticlab.ro/). Strain identification was based on the 16S rRNA gene sequence similarity using the EzTaxon database (http://www.eztaxon.org/). Phylogenetic analyses were conducted using the Molecular Evolutionary Genetics Analysis (MEGA) version 7.0 (Kumar et al., 2016), with bootstrap values generated from 1000 replicates using the Neighbor-Joining method (Saitou & Nei, 1987). The type strain _Cupriavidus necator_ N-1 (DSM 13513) was chosen as a root for the phylogenetic tree. The closest neighbors and type strain from the EzBioCloud database (Yoon et al., 2017) were included in the tree.

2.3 | Confirmation of PHA accumulation

Transmission electron microscopy (TEM) was used for PHA granule visualization. For this, cells were pre-cultured in ASW-Y rich media (supplemented with 5 g/L tryptone), collected by centrifugation, and washed in sterile ASW. Freshly-collected cells were resuspended in ASW without NH_4Cl and supplemented with 2% (w/v) glycerol and 2 g/L urea as carbon and nitrogen sources. The culture (starting at OD_{600} of 0.2) was incubated at 20°C, 150 rpm. For TEM investigation, 1 ml of bacterial culture was harvested at 24 and 72 h. TEM was performed as described elsewhere (Pokrovskaya et al., 2012). Briefly, cells were fixed with 2.5% glutaraldehyde in PHEM buffer (60 mM PIPES, 25 mM HEPES, 10 mM EGTA, 4 mM $MgSO_4 \cdot 7H_2O$), processed and imaged using Hitachi HT7800 TEM with a Xarosa camera (EMSIS GmbH).

2.4 | Growth characteristics and polymer accumulation

The growth dynamics and polymer accumulation were monitored in 250 ml flasks with 100 ml of ASW media supplemented with 1 ml trace element solution, 10 ml vitamin solution, 2% pure glycerol (PG) as sole carbon, and 0.2% urea as the nitrogen source. The flasks were equipped with breather screw caps with ePTFE membranes, for better aeration. Biological replicates were started at OD600 equal to 0.2 and grown for 21 days, at 20°C and 150 rpm. The growth of C2.2 culture was monitored by measuring the optical density at 600 nm (OD_{600}). At each time point, three flasks (biological replicates) were sacrificed, and the cell dry weight (CDW) was determined following the biomass harvesting at 11500 g for 5 min. The pellet was freeze-dried at −55°C (CHRIST ALPHA1-2 LDPlus, Fisher Scientific) and weighed. The total amount and the composition of PHAs were determined following methanolysis of freeze-dried, ground samples. Approximately, 30 mg of dry pellet were subjected to methanolysis with 1.5% sulfuric acid/methanol (3 ml) and chloroform (3 ml) at 100°C for 72 h, in screw-capped test tubes. Benzoic acid (2 mg/test tube) was used as an internal standard. Poly[(R)-3-hydroxybutyric acid] (PHB; #363502, Sigma) was used as positive controls. After

methanolysis, 2 ml of ammonia solution (12.5%) was added to separate the organic and aqueous phases. The organic phase containing methyl ester derivatives was analyzed by a GC-MS system (Varian Saturn 2000) equipped with an HP 5 MS (5%)—diphenyl (95%)—dimethylsiloxane capillary column (30 m, 0.25 mm diameter, 1 µm film thickness). 1 µl sample was injected with 5.0 purity helium as the carrier gas, 13.81 psi, total flow 9 ml/min, column flow 1 ml/min, purge flow 3.0 ml/min, temperature increment of 10°C/min from 50°C to 260°C, injector temperature 220°C. Data analysis was performed using Saturn 2000 MS Workstation.

2.5 | Genomic DNA extraction

Photobacterium ganghwense C2.2 DNA was extracted from cells cultivated on ASW-Y rich media, at 20°C with 150 rpm for 24 h. The extraction was carried out using the PureLink Genomic DNA Extraction kit (Invitrogen, #K1820), according to the manufacturer's instructions. The DNA quantity and quality were evaluated by 0.8% agarose gel electrophoresis and Qubit dsDNA BR assay kit (Life Technologies, #Q32850).

2.6 | Genome sequencing

Sequencing of _P. ganghwense_ C2.2's genome was done at the Functional Genomics Center Zurich (FGCZ, ETH Zurich and the University of Zurich, Switzerland; http://www.fgcz.ch/), using the PacBio RSII platform (Pacific Biosciences). The SMRTbell library was generated using the DNA Template Prep Kit 1.0 (Pacific Biosciences, USA, #100-259-100). The start concentration of the genomic DNA was measured using a Qubit dsDNA BR assay kit (Life Technologies, #Q32850). Then the genomic DNA (5 µg) was mechanically sheared to obtain an average size distribution of 15–20 kb, using a Covaris gTube (Kbiosciences, GB, #520079). Fragment size distribution was assessed using Bioanalyzer 2100 12 K DNA Chip assay (Agilent, #5067-1508). Sheared genomic DNA (5 µg) was DNA-damage repaired and end-repaired using polishing enzymes suggested by the manufacturer. To create the SMRTbell template, a blunt-end ligation reaction was performed, which was then followed by exonuclease treatment. To select the size of the SMRTbell template and enrich for large fragments (>12 kbp) we used a BluePippin device (Sage Science). The size-selected library was quality inspected and quantified on the Agilent Bioanalyzer 12 kb DNA Chip and a Qubit Fluorimeter (Life technologies), respectively. A ready-to sequence SMRT bell-Polymerase Complex was created using the P6 DNA/Polymerase binding kit 2.0 (Pacific Biosciences, #100-236-500) according to the manufacturer's instructions. The Pacific Biosciences RS2 instrument was programmed to load and sequence the sample on one SMRT cell v3.0 (Pacific Biosciences, #100-171-800). A MagBead loading (Pacific Biosciences, #100-133-600) method was chosen to improve the enrichment of the longer fragments.

To assess the adapter dimer contamination, the sample loading efficiency, the obtained average read length, and the number of filtered sub-reads, a sequencing report was generated for every cell, via the SMRT portal. NanoPlot (De Coster et al., 2018) was used to assess the quality of the subreads.

2.7 | Genome assembly

The raw data was initially assembled by the Hierarchical Genome-Assembly Process 3 (HGAP3) pipeline (Pacific Biosciences). The final assembly was done in-house using open-source tools. For this, a subassembly was initially created using the wtdbg2 assembler (Ruan & Li, 2019), with an estimated genome size parameter set at the HGAP3 assembly size value of 5.8 Mbp. The final assembly was generated with the Flye assembler (Kolmogorov et al., 2019) using the wtdbg2-generated subassembly, the HGAP assembly size as a reference, and two rounds of polishing. To assess the completeness of the assembly we used: Bandage (Wick et al., 2015) for graph visualization, Quast (Mikheenko et al., 2018) for obtaining the technical metrics, and BUSCO (Seppey et al., 2019) for evaluating the gene content and presence of single-copy orthologs. Circlator (fixstart; Hunt et al., 2015) was used for changing the start position of the contigs to the origin of replication.

The whole-genome taxonomic affiliation was assessed by in silico genome hybridization with OrthoANI (Lee et al., 2016) to compare the *Photobacterium* C2.2 genome to the existing draft genome of the type strain *P. ganghwense* DSM22954^T (ASM102945v1).

2.8 | Genome annotation

ORF prediction and genome annotation were performed using NCBI PGAP (Prokaryotic Genome Annotation Pipeline). CGView (Stothard & Wishart, 2005) was employed for genome visualization. Besides PGAP annotation, CDS were also functionally annotated via the eggNOG-mapper v2 using the DIAMOND mapping mode (Huerta-Cepas et al., 2017, 2019); KEGG annotation through KoalaBLAST (Kanehisa et al., 2007, 2016); as well as Pathway Tools (Karp et al., 2015) and the integrated PathoLogic annotation tool, with the MetaCyc database (Caspi et al., 2012) for metabolic pathway mapping. For the PHA depolymerase annotation, we used the PHA Depolymerase Engineering Database (Knoll et al., 2009) and BLASTp (Altschul et al., 1990). Annotation quality and genome completeness were verified through a DIAMOND alignment against the UniProt TrEMBL database (Buchfink et al., 2014; Ravintheran et al., 2019; The Uniprot Consortium, 2019; Watson & Warr, 2019). Secondary Metabolite Biosynthetic Gene Clusters (smBGCs) were predicted using antiSMASH v5.0 (Blin et al., 2019). Contigs were screened for antimicrobial and virulence marker genes using Abricate (https://github.com/tseemann/abricate; Seemann, 2017) with the Resfinder database (http://genomicepidemiology.org/; Zankari et al., 2012), and the Virulence Factor Database (VFDB; Liu

et al., 2019), respectively. Prophage regions were identified using PHASTER (Arndt et al., 2016). A workflow of the sequencing, assembly, and annotation processes is presented in Appendix Figure A1.

3 | RESULTS AND DISCUSSION

3.1 | Isolation and characterization of *P. ganghwense* strain C2.2

A total number of 82 bacterial isolates were obtained from the sediment samples. From all the isolates, PHA-production screening done by Nile Red staining highlighted strain C2.2, as its cell fluorescence was observed after 24 h (Figure 1) and maintained throughout the entire incubation period (14-days). Intracellular PHA granule accumulation was demonstrated by TEM imaging after growing the C2.2 in liquid media supplemented with glycerol as a sole carbon source (Figure 1). Cells with numerous small inclusions were already present after 24 h of incubation. After 72 h of incubation, the PHA granules and the cells had shown an apparent growth in size. Enlargement of the cell size may be a mechanism to maximize the capacity for granule storage.

3.2 | 16S rRNA gene sequence and phylogenetic analysis

16S rRNA gene comparison against the EzTaxon database showed the close taxonomical relation of strain C2.2 to members of the *Photobacterium* genera, especially with *P. ganghwense* DSM22954^T. Strain C2.2 shared a 16S rRNA gene sequence similarity of 99.86% and a 99.68% genome identity (see below) with the *P. ganghwense* DSM22954^T type strain. Based on the 16S rRNA gene sequence analysis, the isolated strain was grouped into a distinct cluster, together with two *P. ganghwense* strains, distant from the other three *Photobacterium* species with complete genomic sequences (Figure 2).

3.3 | Polymer accumulation on pure glycerol

Pure glycerol (PG) was used to assess the PHB-production phenotype of strain C2.2. Intracellular polymer accumulation (% CDW) and final PHB production (g/L) were obtained from 2% PG. Culture optical density, CDW, and PHB content increased steadily throughout the cultivation. They stabilized after 7 days (OD$_{600}$ of 33.3 (±0.3)) and remained in close range until the 14th day. Peak values were recorded on the 14th day and reached 65.4% PHB content, with 4 (±0.3) g/L PHB (Figure 3). Strain C2.2 showed the highest overall PHB production (g/L) among those reported for PHA-producing *Gammaproteobacteria* in similar conditions (use of PG as a sole carbon source and shake flask cultivations; see comparative Table 1). This and the moderate halotolerance of the C2.2 strain indicate its suitability for larger-scale PHA-production testing.
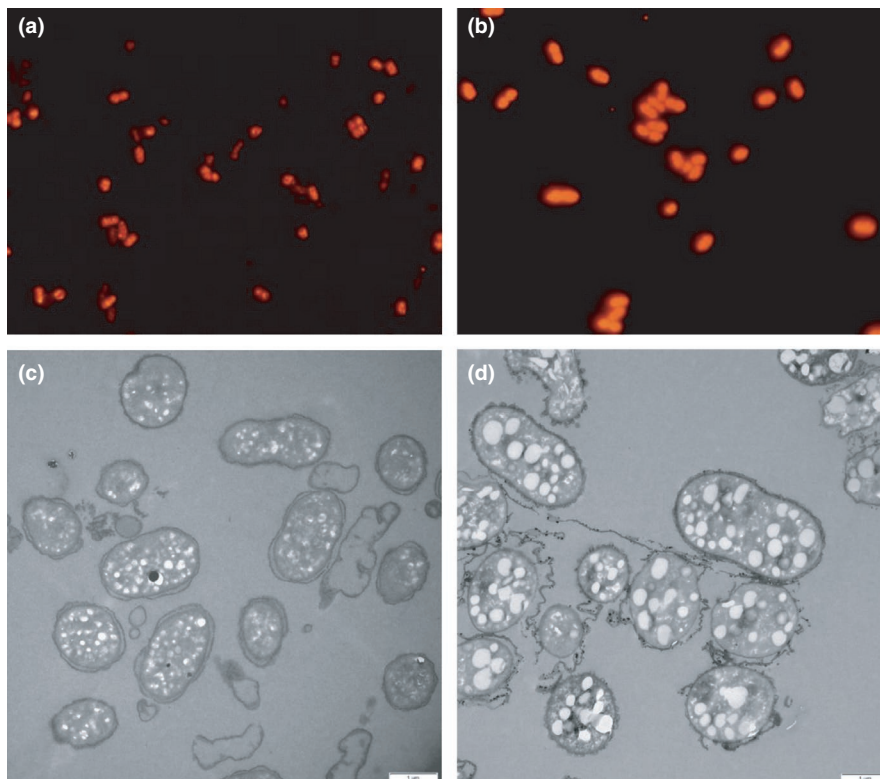
3.4 | Genome of *P. ganghwense* strain C2.2

The genome assembly of *P. ganghwense* stain C2.2 was covered 113x, with a total size of 5,744,420 bp, GC content of 50.34%, and is comprised of two chromosomes and one plasmid (Table 2). Genome comparison of strain C2.2 to the type strain of *P. ganghwense* DSM22954[T] (ASM102945v1) showed an average nucleotide identity of 99.68% further supporting the classification of the C2.2 strain as a member of the *P. ganghwense* species. In terms of genome size, typically, *Photobacterium* species have genomes ranging from 4.2 to 6.4 Mbp, and a GC content between 38.7% and 50.9% (Machado & Gram, 2017). Thus, the 5.74 Mbp size genome and 50.34% GC content of strain C2.2 is similar to that of other metabolically versatile *Photobacterium* species (e.g., *P. profundum* and *P. halotolerans*) and to that of the *P. ganghwense* type strain (ASM102945v1). The C2.2 genome arrangement (Figure 4) into two circular chromosomes is observed for the other two *Photobacterium* species with a complete genomic sequence available and appears specific for the *Vibrionaceae* family (Machado & Gram, 2017). As shown for other species of the genus (Machado & Gram, 2017; Vesth et al., 2010), the second chromosome and the plasmid (202 kbp) can be a source of genomic plasticity and strain-specific differences. In most cases, the studied *Photobacterium* strains have plasmids that range in size from 35 to 80 Kbp (Machado & Gram, 2017). The C2.2 megaplasmid is the second-largest plasmid (202.454 bp) of the genus (the largest—319.190 bp—belonging to *P. damselae* strain Phdp Wu-1; GenBank assembly accession no. GCA_003130755.1).

Genome annotation, by PGAP, yielded 4,983 coding sequences (CDS), 188 tRNAs, 55 rRNAs (Table 3). Assembly completeness evaluation (BUSCO, Appendix Table A2) indicated that single-copy orthologs were 100% and, respectively, 99.6% complete for *Bacteria* and *Vibrionales* lineages. According to the PathoLogic results, the CDS encode for enzymes involved in 304 metabolic pathways. After annotation, a DIAMOND blast against the UniProt TrEMBL database showed that 92.35% of CDS have over 90% similarity to protein sequences from TrEMBL, indicating the sequencing method did not have a negative impact on assembly quality and protein prediction. No CRISPR arrays were annotated.

Genomic basis for PHA accumulation in *P. ganghwense* strain C2.2. The PHA-positive phenotype of strain C2.2. was confirmed by the presence of a complete *phaCAB* operon (Figure 5) via functional annotations of clusters of orthologous groups (COGs). The *phaCAB* is located on chromosome 2, and also includes a *phaP* gene encoding a phasin family protein (FH974_19300), a surface protein with a role in PHA granule stabilization and production (Figure 3). The only annotated *phaC* (FH974_19305) encodes for a class I polyhydroxyalkanoic acid synthase, which polymerizes CoA thioesters of short carbon chain length hydroxyalkanoic acids (C_3-C_5). *phaA* (FH974_19295) and *phaB* (FH974_19290) encode for: acetyl-CoA acetyltransferase—the first enzyme in the PHA synthesis pathway, and an acetoacetyl-CoA reductase. *phaCAB* cluster organization and its similarity of protein sequences with the functional ones of *Cupriavidus necator* H16 (DSM 428; Kutralam-Muniasamy et al., 2018; Figure 5), suggest an operational PHA-synthesis pathway in strain C2.2.

Additionally, three putative *phaP*, four *phaA*, nine *phaB*, and one *phaD*, encoding hypothetical PHA synthesis transcriptional regulators (De Eugenio et al., 2010), were annotated for strain C2.2.
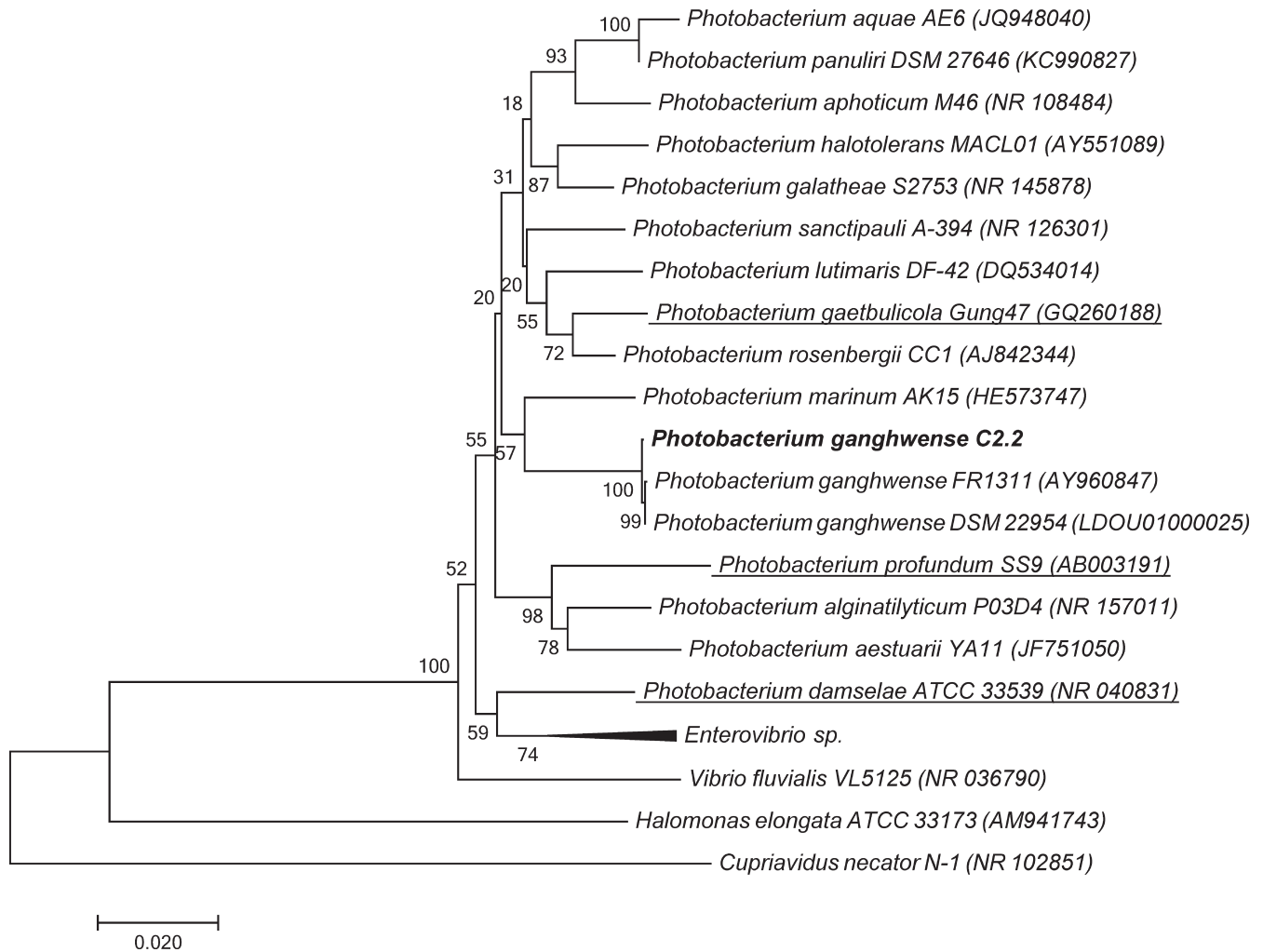
FIGURE 2 16S rRNA gene-based phylogenetic relationships of the "C.2.2" strain. The numbers shown at the tree nodes indicate bootstrap values (in %) based on 1000 replications. The scale bar indicates 0.02 substitutions per nucleotide position. _Photobacterium_ strains with a complete genomic sequence available in public databases are underlined
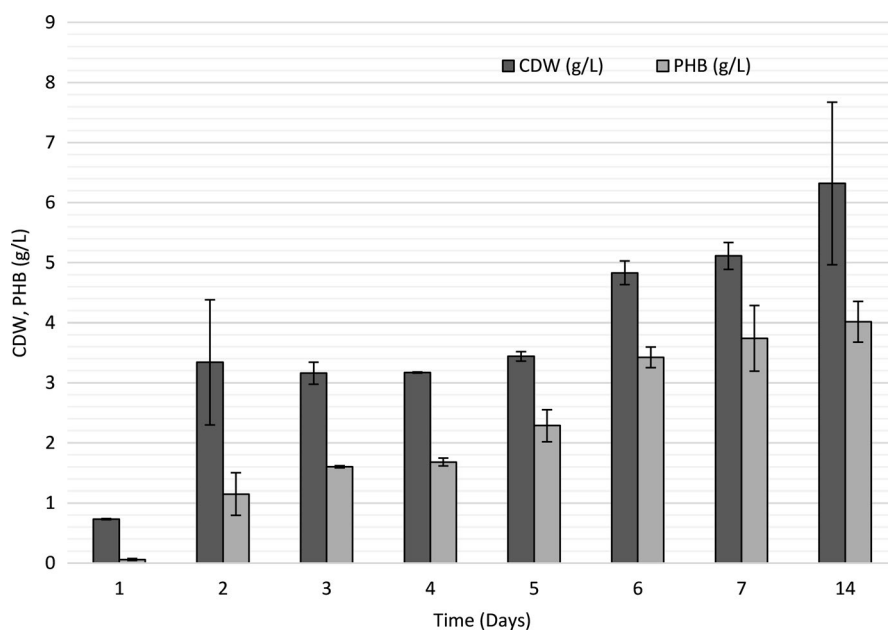

FIGURE 3 Time-dependent cell dry weight (CDW) and PHA accumulation. Changes in _P. ganghwense_ C2.2 cell dry weight (dark gray) and PHA accumulation (light gray; in g/L) when cultivated in shake flasks, on 2% pure glycerol, at 20°C. Bar graphs represent mean values (± SD) of three independent experiments

TABLE 1 Production of PHA from pure glycerol by *Gammaproteobacteria* strains and *Cupriavidus necator*

Strain	Time (h)	Culture volume (ml)[a]	Pure glycerol (%; v:v)	CDW (g/L)	PHA content (% of CDW)	References
Photobacterium ganghwense C2.2	96 14 days	100	2	3.1 6.3	53 65.4	Current study
Vibrio harveyi MCCB 284	72	200	2	3	68	Mohandas et al. (2017)
Vibrio spp. M11/M14/M20/M31	24 h after stationary phase	200	1	0.31/0.31/0.44/0.45	30.2/31.5/42.8/24	Chien et al. (2007)
Vibrio proteolyticus	48	NM	1	~ 1.6	<10	Hong et al. (2019)
Salinivibrio sp. M318	48	50	3	7.2	39	Van Thuoc et al. (2019)
Zobellella denitrificans MW1	100	300	2	3.7	73.5	Ibrahim and Steinbüchel (2010)
Aeromonas spp. AC_01/AC_02/AC_03	48	NM	1	1.69/1.48/1.2	7.8/5/3.6	Możejko-Ciesielska and Pokoj (2018)
Halomonas sp. KM-1	60	20	2	NM	40.5	Kawata and Aiba (2010)
Cupriavidus necator DSM 545[b]	88	100	2 3	~6.35 ~7.18	~77 ~79	Sun et al. (2020)
Cupriavidus necator DSM 545[b]	33.5	Fed-batch 1500	24.9	82.5	62	Cavalheiro et al. (2009)

A PHB content (wt%) was expressed as a percentage of PHA mass in dry cell mass.

Abbreviation: NM, not mentioned.

[a]The culture volume in shake flask, if not mentioned otherwise.; [b]*Cupriavidus necator* DSM 545 is used in the industrial production of PHA.

TABLE 2 The metrics for the *in-house* Flye assembly generated with QUAST

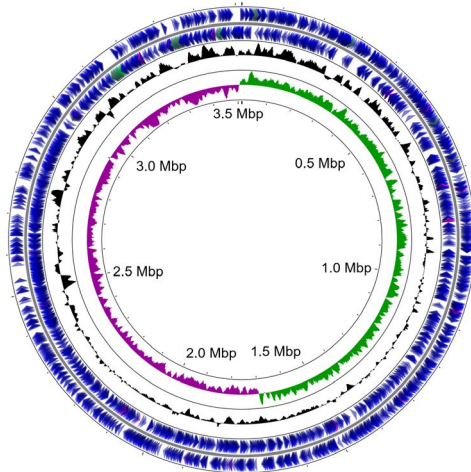| Assembly metrics		Assembly metrics	
# contigs	3	GC (%)	50.34
Contig 1 length (bp)	3,515,384	N50	3,515,384
Contig 2 length (bp)	2,026,582	N75	2,026,582
Contig 3 length (bp)	202,454	Avg. coverage depth	113
Total length	5,744,420	# N's per 100 kbp	0

Unlike other PHA-producing bacteria, genes encoding the PHA-dependent transcriptional regulatory proteins (*phaR/Q/F*) and PHA depolymerase (*phaZ*) were not identified in the genome of *P. ganghwense* strain C2.2. The absence of PHA depolymerase was validated via a BLASTp search against the PHA Depolymerase Engineering Database (http://www.ded.uni-stuttgart.de/; DED). This finding may explain the prolonged stability of accumulated PHB in the shake flask experiments (Figure 3). In a recent paper, de Vogel et al. (2021) highlighted similar features for two *Vibrio* strains (*V. proteolyticus* ATCC 15338 and *V. alginolyticus* ATCC 33787) that lack sequences similar to PhaZ depolymerases. For those strains, the authors re-assigned two initially annotated lipases as putative extracellular PHA depolymerases. The putative depolymerases were found to be most similar to the PhaZ7 depolymerase present in *Paucimonas lemoignei*, with demonstrated depolymerase activity for extracellular amorphous PHA (native PHA granules; Handrick et al., 2001). A BLASTp hit similar to this supposed extracellular depolymerases (92% coverage, 82%–84% identity) was found in the genome of *Photobacterium* sp. C2.2 (FH974_07335). Its presence may indicate the ability of strain C2.2 to degrade PHB only after PHB's extracellular release succeeding the cell death. The confirmation of depolymerase activity for this putative lipase needs to be addressed in future experiments.

In contrast, *C. necator* H16, the model strain for PHA production studies, has five well-characterized intracellular and two extracellular depolymerases, as well as two oligomer hydrolases (Brigham et al., 2012). The absence of a depolymerase may prove advantageous for biotechnological applications, as PHA-producing strains are usually genetically engineered to inactivate the depolymerization step for a higher yield in PHA production and increase the PHA molecular mass (Adaya et al., 2018; Kadouri et al., 2003; Kobayashi & Kondo, 2019).
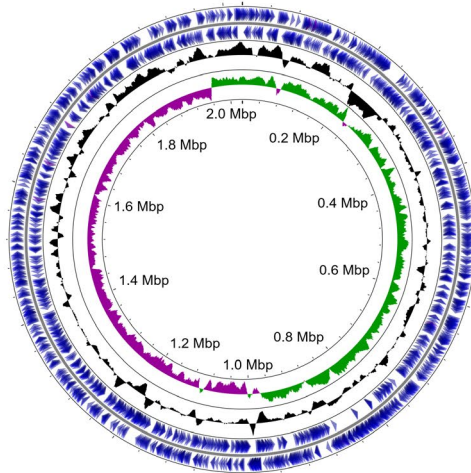
Likewise, except for the extracellular PHA oligomer hydrolase PhaY, all the genes for enzymes involved in the catabolism of

Accession: CP071325
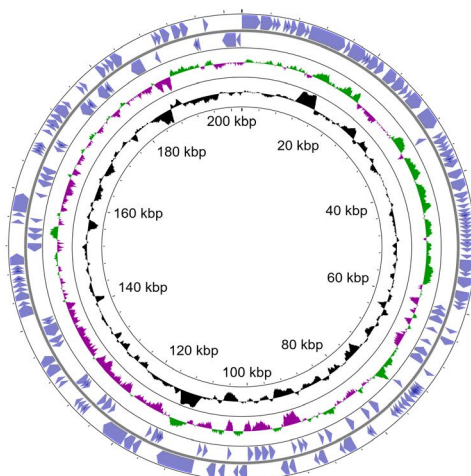
Photobacterium ganghwense
strain C2.2

FIGURE 4 The two chromosomes
and plasmid of *P. ganghwense* strain C2.2.
The genome maps consist of genome
information displayed circularly (from
the outside in): CDS, tRNA, rRNA, G + C
content, and GC skew

- CDS
- tRNA
- rRNA
- GC Content
- GC Skew+
- GC Skew-

Chromosome 1

Accession: CP071326

- CDS
- tRNA
- GC Content
- GC Skew+
- GC Skew-

Chromosome 2

Accession: CP071327

- CDS
- GC Skew+
- GC Skew-
- GC Content

Plasmid pPGC22

TABLE 3 Genome features for strain C2.2

Features		Features	
Genome size (bp)	5,744,420	CDS (coding)	4.875
Chromosome	2	tRNAs	188
Plasmid	1	rRNAs	55
Genes	5.198	ncRNAs	4
CDS (total)	4.951	Pseudogenes	76

hydroxyacyl monomers were annotated in strain C2.2 genome: FabG (FH974_05790, FH974_24585), acetoacetate CoA synthetase AacS (FH974_21375), 3-oxoacid-CoA-transferase subunits A and B (ScoA - FH974_04750; ScoB - FH974_04745, FH974_24545), and 3-hydroxyisobutyrate dehydrogenase MmsB (FH974_21025).

As expected, strain C2.2. harbored all four genes (*glpK*, *glpD*, *glpC*, *glpB*) of the glycerol conversion pathway: *glpK* (FH974_00925) encodes for a glycerol kinase that converts glycerol to glycerol 3-phosphate; *glpD* (FH974_00520) encodes for a glycerol-3-phosphate dehydrogenase that converts glycerol 3-phosphate to dihydroxyacetone phosphate, which feeds into the glycolysis pathway, where it ultimately becomes acetyl-CoA, a substrate for PHB synthesis (Kok et al., 1998); *glpC* (FH974_06490), and *glpB* (FH974_06495) encode subunits for an anaerobic glycerol-3-phosphate dehydrogenase (Cole et al., 1988).

Previous studies have shown the efficient use of glycerol for PHA production (Phithakrotchanakoon et al., 2015; Rodríguez-Contreras et al., 2015; Tanadchangsaeng & Yu, 2012). In the case of *C. necator* H16, when glycerol was used instead of expensive sugars (e.g., glucose), the molecular weight of the resulting polymer was reduced, but its thermal and mechanical properties remained unchanged (Tanadchangsaeng & Yu, 2012).

Other pathways. Several metabolic pathways of biotechnological interest were annotated: a complete pathway for the degradation of phenylacetate (Teufel et al., 2010) to acetyl CoA, with a total of 51 genes involved in the degradation and metabolism of xenobiotics; complete pathways for the synthesis of various isoprenoids; genes involved in the metabolism of various terpenoids and polyketides; pathways for the degradation of various carbohydrates, such as starch, glycogen, chitin, etc. Such metabolic versatility could prove useful in expanding the range of raw substrates for the production of PHAs.

Prediction of smBGCs. Secondary metabolites have great potential for biotechnological applications (e.g., antibiotics, pigments,

growth hormones, antitumor agents, and others). Since the production of bioactive molecules is poorly studied in *Photobacterium* (Čihák et al., 2017), we screened the genome of strain C2.2 for putative smBGCs. Based on their homology to known smBGCs, we predicted seven such gene clusters: four smBGCs on the large chromosome and three on the small chromosome. Strain C2.2 megaplasmid CDSs included no smBGCs nor genes involved in horizontal gene transfer. The smBGCs identified on the larger chromosome encode for antimicrobial functions: bacteriocin (FH974_15530), thiopeptide (FH974_04020 - FH974_04040), and betalactone (FH974_13860 - FH974_13885). These compounds provide a competitive advantage and protection from other microbial community members but could also mediate interspecies interactions (Čihák et al., 2017). The smBGCs identified on the smaller chromosome encode for: ectoine (*ectABC* operon), aryl polyene (T2PKS; FH974_24595), and polyketide (T1PKS; FH974_21825) synthesis. Polyketides like aryl polyene pigments are broadly distributed within Bacteria (Grammbitter et al., 2019). Polyketides, together with ectoine, serve as protection against reactive oxygen species and may have a protective role for strain C2.2 in marine environments (Das et al., 2015; Schöner et al., 2016). Further research is needed to investigate whether there is a link between the production of these compounds and certain environmental conditions.

Antimicrobial susceptibilities and resistance genes. Since many strains of the *Photobacterium* genus are well known for their virulence and antimicrobial resistance (Chiu et al., 2013; Fuertes-Perez et al., 2019; Labella et al., 2017; Nonaka et al., 2012), we screened the *P. ganghwense* C2.2 genome for the acquired resistance mechanisms using Abricate. Surprisingly, strain C2.2 had only one antibiotic resistance gene (*qnrS5*) associated with resistance to fluoroquinolone (Han et al., 2012).

Abricate revealed several putative virulence-associated genes: *cheW*-2 chemotaxis protein, *fli*G—flagellar motor protein, *fli*M, and *fli*N, both polar flagellar switch proteins, involved in cell signaling and motility in liquid environments. These genes represent only a small fraction of the 15 core virulence genes of *Gammaproteobacteria* (Vázquez-Rosas-Landa et al., 2017).

Acquisition of additional virulence genes by horizontal gene transfer could be possibly mediated by one of the five phage regions predicted by PHASTER (Srividhya et al., 2007; Vázquez-Rosas-Landa et al., 2017). However, all five prophage regions are incomplete, with the largest being 103 kb in length and located on the small chromosome.
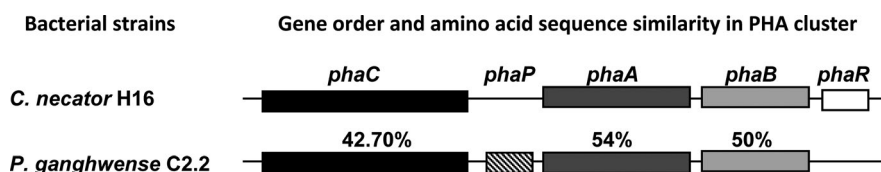
Bacterial strains	Gene order and amino acid sequence similarity in PHA cluster

FIGURE 5 Simplified comparative analysis of PHA gene clusters from the PHA model organism *C. necator* H16 and *P. ganghwense* C2.2. The coding regions are indicated as follows: PHA synthase gene *phaC* (black); precursor-generating enzymes genes *phaA* (dark gray) and *phaB* (light gray); surface protein gene *phaP* (oblique lines); PHA dependent transcriptional regulator *phaR* (white). The numbers above the coding regions indicate the sequence similarities with the protein counterparts of *C. necator* H16

Auspiciously, a low number of antibiotic resistance and virulence genes along with the incomplete prophage regions are an indicator of genome stability, which may be beneficial in the potential biotechnological applications of _P. ganghwense_ strain C2.2.

4 | CONCLUSIONS

We obtained the first complete genomic sequence for a _Photobacterium ganghwense_ strain. Moreso, strain C2.2 is capable of using glycerol, as a sole carbon source, to produce PHA granules. Genome analysis revealed the presence of all the genes required to synthesize PHA from glycerol, supporting the PHA-producing phenotype. Observation of PHA accumulation dynamics showed a sustained increase in PHA content, with peak CDW and PHB content on day 14th. Gene annotation indicated the lack of a PHA depolymerase in the strain C2.2 genome. Although a putative lipase with the presumed ability to degrade extracellular amorphous PHA was annotated, our findings suggest that strain C2.2 is naturally prone to accumulate PHA for extended periods, a feature of great biotechnological importance. Also, the multitude of secondary metabolic pathways combined with the low number of genes involved in antibiotic resistance and virulence can be a plus from an applied science perspective. Our findings highlight the biotechnological potential of _P. ganghwense_ strain C2.2, increasing the existing knowledge regarding PHA-producing bacteria. The complete genome of a _Photobacterium ganghwense_ contributes to the understanding of the _Photobacterium_ genus.

AUTHOR CONTRIBUTIONS
Irina Andreea Lascu: Data curation (equal); Formal analysis (equal); Investigation (equal); Methodology (equal); Validation (equal); Writing-original draft (equal). **Ioana Mereuta:** Data curation (equal); Formal analysis (equal); Investigation (equal); Methodology (equal); Validation (equal); Writing-original draft (equal). **Iulia Chiciudean:** Conceptualization (equal); Investigation (equal); Writing-original draft (equal); Writing-review & editing (lead). **Hilde Hansen:** Investigation (equal); Writing-original draft (equal); Writing-review & editing (equal). **Sorin Marius Avramescu:** Investigation (equal); Writing-original draft (supporting). **Ana-Maria Tanase:** Conceptualization (equal); Funding acquisition (lead); Project administration (lead); Writing-original draft (equal). **Ileana Stoica:** Supervision (supporting).

ORCID
Iulia Chiciudean https://orcid.org/0000-0003-3180-2578

REFERENCES
Abushattal, S., Vences, A., & Osorio, C. R. (2020). A virulence gene typing scheme for _Photobacterium damselae_ subsp. _piscicida_, the causative agent of fish photobacteriosis, reveals a high prevalence of plasmid-encoded virulence factors and of type III secretion system genes. _Aquaculture_, _521_, 735057. https://doi.org/10.1016/j.aquaculture.2020.735057

Adaya, L., Millán, M., Peña, C., Jendrossek, D., Espín, G., Tinoco-Valencia, R., Guzmán, J., Pfeiffer, D., & Segura, D. (2018). Inactivation of an intracellular poly-3-hydroxybutyrate depolymerase of _Azotobacter vinelandii_ allows to obtain a polymer of uniform high molecular mass. _Applied Microbiology and Biotechnology_, _102_(6), 2693–2707. https://doi.org/10.1007/s00253-018-8806-y

Alcântara, J. M. G., Distante, F., Storti, G., Moscatelli, D., Morbidelli, M., & Sponchioni, M. (2020). Current trends in the production of biodegradable bioplastics: The case of polyhydroxyalkanoates. _Biotechnology Advances_, _42_, 107582. https://doi.org/10.1016/j.biotechadv.2020.107582

Altschul, S. F., Gish, W., Miller, W., Myers, E. W., & Lipman, D. J. (1990). Basic local alignment search tool. _Journal of Molecular Biology_, _215_(3), 403–410. https://doi.org/10.1016/S0022-2836(05)80360-2

Arndt, D., Grant, J. R., Marcu, A., Sajed, T., Pon, A., Liang, Y., & Wishart, D. S. (2016). PHASTER: A better, faster version of the PHAST phage search tool. _Nucleic Acids Research_, _44_(W1), W16–W21. https://doi.org/10.1093/nar/gkw387

Blin, K., Shaw, S., Steinke, K., Villebro, R., Ziemert, N., Lee, S. Y., Medema, M. H., & Weber, T. (2019). AntiSMASH 5.0: Updates to the secondary metabolite genome mining pipeline. _Nucleic Acids Research_, _47_(W1), W81–W87. https://doi.org/10.1093/nar/gkz310

Boyandin, A. N., Kalacheva, G. S., Rodicheva, E. K., & Volova, T. G. (2008). Synthesis of reserve polyhydroxyalkanoates by luminescent bacteria. *Microbiology*, 77(3), 318–323. https://doi.org/10.1134/S0026261708030119

Brigham, C. J., Reimer, E. N., Rha, C. K., & Sinskey, A. J. (2012). Examination of PHB depolymerases in *Ralstonia eutropha*: Further elucidation of the roles of enzymes in PHB homeostasis. *AMB Express*, 2(1), 26. https://doi.org/10.1186/2191-0855-2-26

Buchfink, B., Xie, C., & Huson, D. H. (2015). Fast and sensitive protein alignment using DIAMOND. *Nature Methods*, 12(1), 59–60. https://doi.org/10.1038/nmeth.3176

Caspi, R., Altman, T., Dreher, K., Fulcher, C. A., Subhraveti, P., Keseler, I. M., Kothari, A., Krummenacker, M., Latendresse, M., Mueller, L. A., Ong, Q., Paley, S., Pujar, A., Shearer, A. G., Travers, M., Weerasinghe, D., Zhang, P., & Karp, P. D. (2012). The MetaCyc database of metabolic pathways and enzymes and the BioCyc collection of pathway/genome databases. *Nucleic Acids Research*, 40(D1), 742–753. https://doi.org/10.1093/nar/gkr1014

Cavaillé, L., Albuquerque, M., Grousseau, E., Lepeuple, A.-S., Uribelarrea, J.-L., Hernandez-Raquet, G., & Paul, E. (2016). Understanding of polyhydroxybutyrate production under carbon and phosphorus-limited growth conditions in non-axenic continuous culture. *Bioresource Technology*, 201, 65–73. https://doi.org/10.1016/j.biortech.2015.11.003

Cavalheiro, J. M. B. T., de Almeida, M. C. M. D., Grandfils, C., & da Fonseca, M. M. R. (2009). Poly(3-hydroxybutyrate) production by *Cupriavidus necator* using waste glycerol. *Process Biochemistry*, 44(5), 509–515. https://doi.org/10.1016/j.procbio.2009.01.008

Chae, Y., & An, Y.-J. (2018). Current research trends on plastic pollution and ecological impacts on the soil ecosystem: A review. *Environmental Pollution*, 240, 387–395. https://doi.org/10.1016/j.envpol.2018.05.008

Chien, C. C., Chen, C. C., Choi, M. H., Kung, S. S., & Wei, Y. H. (2007). Production of poly-β-hydroxybutyrate (PHB) by *Vibrio* spp. isolated from marine environment. *Journal of Biotechnology*, 132(3), 259–263. https://doi.org/10.1016/j.jbiotec.2007.03.002

Chiu, T.-H., Kao, L.-Y., & Chen, M.-L. (2013). Antibiotic resistance and molecular typing of *Photobacterium damselae* subsp. *damselae*, isolated from seafood. *Journal of Applied Microbiology*, 114(4), 1184–1192. https://doi.org/10.1111/jam.12104

Čihák, M., Kameník, Z., Šmídová, K., Bergman, N., Benada, O., Kofroňová, O., Petříčková, K., & Bobek, J. (2017). Secondary metabolites produced during the germination of *Streptomyces coelicolor*. *Frontiers in Microbiology*, 8, 2495. https://doi.org/10.3389/fmicb.2017.02495

Cole, S. T., Eiglmeier, K., Ahmed, S., Honore, N., Elmes, L., Anderson, W. F., & Weiner, J. H. (1988). Nucleotide sequence and gene-polypeptide relationships of the glpABC operon encoding the anaerobic sn-glycerol-3-phosphate dehydrogenase of *Escherichia coli* K-12. *Journal of Bacteriology*, 170(6), 2448–2456. https://doi.org/10.1128/jb.170.6.2448-2456.1988

Das, P., Behera, B. K., Kumar Meena, D., Syed, A., Azmi, S., Chatterjee, S., Meena, K., & Sharma, A. (2015). Salt stress tolerant genes in halophilic and halotolerant bacteria: Paradigm for salt stress adaptation and osmoprotection. *International Journal of Current Microbiology and Applied Sciences*, 4(1), 642–658.

De Coster, W., D'Hert, S., Schultz, D. T., Cruts, M., & Van Broeckhoven, C. (2018). NanoPack: Visualizing and processing long-read sequencing data. *Bioinformatics*, 34(15), 2666–2669. https://doi.org/10.1093/bioinformatics/bty149

De Eugenio, L. I., Galán, B., Escapa, I. F., Maestro, B., Sanz, J. M., García, J. L., & Prieto, M. A. (2010). The PhaD regulator controls the simultaneous expression of the pha genes involved in polyhydroxyalkanoate metabolism and turnover in *Pseudomonas putida* KT2442. *Environmental Microbiology*, 12(6), 1591–1603. https://doi.org/10.1111/j.1462-2920.2010.02199.x

De Kok, A., Hengeveld, A. F., Martin, A., & Westphal, A. H. (1998). The pyruvate dehydrogenase multi-enzyme complex from Gram-negative bacteria. *Biochimica Et Biophysica Acta (BBA) - Protein Structure and Molecular Enzymology*, 1385(2), 353–366. https://doi.org/10.1016/S0167-4838(98)00079-X

de Vogel Fons A., Schlundt Cathleen, Stote Robert E., Ratto Jo Ann, Amaral-Zettler Linda A. (2021). Comparative Genomics of Marine Bacteria from a Historically Defined Plastic Biodegradation Consortium with the Capacity to Biodegrade Polyhydroxyalkanoates. *Microorganisms*, 9(1), 186. http://dx.doi.org/10.3390/microorganisms9010186

El-malek, F. A., Khairy, H., Farag, A., & Omar, S. (2020). The sustainability of microbial bioplastics, production and applications. *International Journal of Biological Macromolecules*, 157, 319–328. https://doi.org/10.1016/j.ijbiomac.2020.04.076

Eriksen, M., Lebreton, L. C. M. M., Carson, H. S., Thiel, M., Moore, C. J., Borerro, J. C., Galgani, F., Ryan, P. G., & Reisser, J. (2014). Plastic pollution in the World's Oceans: More than 5 trillion plastic pieces weighing over 250,000 tons afloat at Sea. *PLoS One*, 9(12), 1–15. https://doi.org/10.1371/journal.pone.0111913

Fuertes-Perez, S., Hauschild, P., Hilgarth, M., & Vogel, R. F. (2019). Biodiversity of *Photobacterium* spp. isolated from meats. *Frontiers in Microbiology*, 10, 2399. https://doi.org/10.3389/fmicb.2019.02399

Fumanal, M., Di Zeo, D. E., Anguís, V., Fernández-Diaz, C., Alarcón, F. J., Piñera, R., Albaladejo-Riad, N., Esteban, M. A., Moriñigo, M. A., & Balebona, M. C. (2020). Inclusion of dietary *Ulva ohnoi* 5% modulates *Solea senegalensis* immune response during *Photobacterium damselae* subsp. *piscicida* infection. *Fish and Shellfish Immunology*, 100, 186–197. https://doi.org/10.1016/j.fsi.2020.03.007

Gahlawat, G., & Soni, S. K. (2017). Valorization of waste glycerol for the production of poly (3-hydroxybutyrate) and poly (3-hydroxybutyrate-co-3-hydroxyvalerate) copolymer by *Cupriavidus necator* and extraction in a sustainable manner. *Bioresource Technology*, 243, 492–501. https://doi.org/10.1016/j.biortech.2017.06.139

Grammbitter, G. L. C., Schmalhofer, M., Karimi, K., Shi, Y. M., Schöner, T. A., Tobias, N. J., Morgner, N., Groll, M., & Bode, H. B. (2019). An uncommon type II PKS catalyzes biosynthesis of aryl polyene pigments. *Journal of the American Chemical Society*, 141(42), 16615–16623. https://doi.org/10.1021/jacs.8b10776

Han, J. E., Kim, J. H., Cheresca, C. H., Shin, S. P., Jun, J. W., Chai, J. Y., Han, S. Y., & Park, S. C. (2012). First description of the qnrS-like (qnrS5) gene and analysis of quinolone resistance-determining regions in motile *Aeromonas* spp. from diseased fish and water. *Research in Microbiology*, 163(1), 73–79. https://doi.org/10.1016/j.resmic.2011.09.001

Handrick, R., Reinhardt, S., Focarete, M. L., Scandola, M., Adamus, G., Kowalczuk, M., & Jendrossek, D. (2001). A new type of thermoalkalophilic hydrolase of *Paucimonas lemoignei* with high specificity for amorphous polyesters of short chain-length hydroxyalkanoic acids. *Journal of Biological Chemistry*, 276(39), 36215–36224. https://doi.org/10.1074/jbc.M101106200

Harding, K. G., Dennis, J. S., von Blottnitz, H., & Harrison, S. T. L. (2007). Environmental analysis of plastic production processes: Comparing petroleum-based polypropylene and polyethylene with biologically-based poly-β-hydroxybutyric acid using life cycle analysis. *Journal of Biotechnology*, 130(1), 57–66. https://doi.org/10.1016/j.jbiotec.2007.02.012

Haward, M. (2018). Plastic pollution of the world's seas and oceans as a contemporary challenge in ocean governance. *Nature Communications*, 9(1), 667. https://doi.org/10.1038/s41467-018-03104-3

Hong, J.-W., Song, H.-S., Moon, Y.-M., Hong, Y.-G., Bhatia, S. K., Jung, H.-R., Choi, T.-R., Yang, S.-Y., Park, H.-Y., Choi, Y.-K., & Yang, Y.-H. (2019). Polyhydroxybutyrate production in halophilic marine bacteria *Vibrio proteolyticus* isolated from the Korean peninsula.

Bioprocess and Biosystems Engineering, *42*(4), 603–610. https://doi.org/10.1007/s00449-018-02066-6

Huerta-Cepas, J., Forslund, K., Coelho, L. P., Szklarczyk, D., Jensen, L. J., von Mering, C., & Bork, P. (2017). Fast genome-wide functional annotation through orthology assignment by eggNOG-mapper. *Molecular Biology and Evolution*, *34*(8), 2115–2122. https://doi.org/10.1093/molbev/msx148

Huerta-Cepas, J., Szklarczyk, D., Heller, D., Hernández-Plaza, A., Forslund, S. K., Cook, H., Mende, D. R., Letunic, I., Rattei, T., Jensen, L. J., von Mering, C., & Bork, P. (2019). eggNOG 5.0: A hierarchical, functionally and phylogenetically annotated orthology resource based on 5090 organisms and 2502 viruses. *Nucleic Acids Research*, *47*(D1), D309–D314. https://doi.org/10.1093/nar/gky1085

Hunt, M., Silva, N. D., Otto, T. D., Parkhill, J., Keane, J. A., & Harris, S. R. (2015). Circlator: Automated circularization of genome assemblies using long sequencing reads. *Genome Biology*, *16*(1), 294. https://doi.org/10.1186/s13059-015-0849-0

Ibrahim, M. H. A., & Steinbüchel, A. (2010). *Zobellella denitrificans* strain MW1, a newly isolated bacterium suitable for poly(3-hydroxybutyrate) production from glycerol. *Journal of Applied Microbiology*, *108*(1), 214–225. https://doi.org/10.1111/j.1365-2672.2009.04413.x

Inoue, D., Suzuki, Y., Uchida, T., Morohoshi, J., & Sei, K. (2016). Polyhydroxyalkanoate production potential of heterotrophic bacteria in activated sludge. *Journal of Bioscience and Bioengineering*, *121*(1), 47–51. https://doi.org/10.1016/j.jbiosc.2015.04.022

Kadouri, D., Jurkevitch, E., & Okon, Y. (2003). Poly β-hydroxybutyrate depolymerase (PhaZ) in *Azospirillum brasilense* and characterization of a phaZ mutant. *Archives of Microbiology*, *180*(5), 309–318. https://doi.org/10.1007/s00203-003-0590-z

Kanehisa, M., Araki, M., Goto, S., Hattori, M., Hirakawa, M., Itoh, M., Katayama, T., Kawashima, S., Okuda, S., Tokimatsu, T., & Yamanishi, Y. (2007). KEGG for linking genomes to life and the environment. *Nucleic Acids Research*, *36*(Database), D480–D484. https://doi.org/10.1093/nar/gkm882

Kanehisa, M., Sato, Y., & Morishima, K. (2016). BlastKOALA and GhostKOALA: KEGG tools for functional characterization of genome and metagenome sequences. *Journal of Molecular Biology*, *428*(4), 726–731. https://doi.org/10.1016/j.jmb.2015.11.006

Karp, P. D., Paley, S. M., Midford, P. E., Krummenacker, M., Billington, R., Kothari, A., Ong, W. K., Subhraveti, P., Keseler, I. M., & Caspi, R. (2015). Pathway Tools version 23.0: Integrated Software for Pathway/Genome Informatics and Systems Biology. *Briefings in Bioinformatics*, *11*(1), 40–79.

Kawata, Y., & Aiba, S. I. (2010). Poly(3-hydroxybutyrate) production by isolated *Halomonas* sp. KM-1 using waste glycerol. *Bioscience, Biotechnology and Biochemistry*, *74*(1), 175–177. https://doi.org/10.1271/bbb.90459

Keshavarz, T., & Roy, I. (2010). Polyhydroxyalkanoates: Bioplastics with a green agenda. *Current Opinion in Microbiology*, *13*(3), 321–326. https://doi.org/10.1016/j.mib.2010.02.006

Knoll, M., Hamm, T. M., Wagner, F., Martinez, V., & Pleiss, J. (2009). The PHA depolymerase engineering database: A systematic analysis tool for the diverse family of polyhydroxyalkanoate (PHA) depolymerases. *BMC Bioinformatics*, *10*(1), 1–8. https://doi.org/10.1186/1471-2105-10-89

Kobayashi, J., & Kondo, A. (2019). Disruption of poly (3-hydroxyalkanoate) depolymerase gene and overexpression of three poly (3-hydroxybutyrate) biosynthetic genes improve poly (3-hydroxybutyrate) production from nitrogen rich medium by *Rhodobacter sphaeroides*. *Microbial Cell Factories*, *18*(1), 40. https://doi.org/10.1186/s12934-019-1088-y

Koller, M., Gasser, I., Schmid, F., & Berg, G. (2011). Linking ecology with economy: Insights into polyhydroxyalkanoate-producing microorganisms. *Engineering in Life Sciences*, *11*(3), 222–237. https://doi.org/10.1002/elsc.201000190

Koller, M., & Marsalek, L. (2015). Principles of glycerol-based polyhydroxyalkanoate production. *Applied Food Biotechnology*, *2*(4), 3–10.

Kolmogorov, M., Yuan, J., Lin, Y., & Pevzner, P. A. (2019). Assembly of long, error-prone reads using repeat graphs. *Nature Biotechnology*, *37*(5), 540–546. https://doi.org/10.1038/s41587-019-0072-8

Kumar, S., Stecher, G., & Tamura, K. (2016). MEGA7: Molecular evolutionary genetics analysis version 7.0 for bigger datasets. *Molecular Biology and Evolution*, *33*(7), 1870–1874. https://doi.org/10.1093/molbev/msw054

Kutralam-Muniasamy, G., Marsch, R., & Pérez-Guevara, F. (2018). Investigation on the evolutionary relation of diverse polyhydroxyalkanoate gene clusters in *Betaproteobacteria*. *Journal of Molecular Evolution*, *86*(7), 470–483. https://doi.org/10.1007/s00239-018-9859-3

Labella, A. M., Arahal, D. R., Castro, D., Lemos, M. L., & Borrego, J. J. (2017). Revisiting the genus *Photobacterium*: Taxonomy, ecology and pathogenesis the only species described in the. *International Microbiology*, *20*(1), 1–10. https://doi.org/10.2436/20.1501.01.280

Lee, I., Ouk Kim, Y., Park, S.-C., & Chun, J. (2016). OrthoANI: An improved algorithm and software for calculating average nucleotide identity. *International Journal of Systematic and Evolutionary Microbiology*, *66*(2), 1100–1103. https://doi.org/10.1099/ijsem.0.000760

Liu, B., Zheng, D., Jin, Q., Chen, L., & Yang, J. (2019). VFDB 2019: A comparative pathogenomic platform with an interactive web interface. *Nucleic Acids Research*, *47*(D1), D687–D692. https://doi.org/10.1093/nar/gky1080

Machado, H., & Gram, L. (2017). Comparative genomics reveals high genomic diversity in the genus *Photobacterium*. *Frontiers in Microbiology*, *8*(1204), 1–14. https://doi.org/10.3389/fmicb.2017.01204

Mikheenko, A., Prjibelski, A., Saveliev, V., Antipov, D., & Gurevich, A. (2018). Versatile genome assembly evaluation with QUAST-LG. *Bioinformatics*, *34*(13), i142–i150. https://doi.org/10.1093/bioinformatics/bty266

Mohandas, S. P., Balan, L., Lekshmi, N., Cubelio, S. S., Philip, R., & Bright Singh, I. S. (2017). Production and characterization of polyhydroxybutyrate from *Vibrio harveyi* MCCB 284 utilizing glycerol as carbon source. *Journal of Applied Microbiology*, *122*(3), 698–707. https://doi.org/10.1111/jam.13359

Możejko-Ciesielska, J., & Pokoj, T. (2018). Exploring nutrient limitation for polyhydroxyalkanoates synthesis by newly isolated strains of *Aeromonas* sp. using biodiesel-derived glycerol as a substrate. *PeerJ*, *2018*(10), e5838. https://doi.org/10.7717/peerj.5838

Muhammadi, Shabina, Afzal, M., & Hameed, S. (2015). Bacterial polyhydroxyalkanoates-eco-friendly next generation plastic: Production, biocompatibility, biodegradation, physical properties and applications. *Green Chemistry Letters and Reviews*, *8*(3–4), 56–77. https://doi.org/10.1080/17518253.2015.1109715

Noda, I., Green, P. R., Satkowski, M. M., & Schechtman, L. A. (2005). Preparation and properties of a novel class of polyhydroxyalkanoate copolymers. *Biomacromolecules*, *6*(2), 580–586. https://doi.org/10.1021/bm049472m

Nonaka, L., Maruyama, F., Miyamoto, M., Miyakoshi, M., Kurokawa, K., & Masuda, M. (2012). Novel conjugative transferable multiple drug resistance plasmid pAQU1 from *Photobacterium damselae* subsp. *damselae* isolated from marine aquaculture environment. *Microbes and Environments*, *27*(3), 263–272. https://doi.org/10.1264/jsme2.ME11338

Park, Y.-D., Baik, K. S., Seong, C. N., Bae, K. S., Kim, S., & Chun, J. (2006). *Photobacterium ganghwense* sp. nov., a halophilic bacterium isolated from sea water. *International Journal of Systematic and Evolutionary Microbiology*, *56*(4), 745–749. https://doi.org/10.1099/ijs.0.63811-0

Phithakrotchanakoon, C., Champreda, V., Aiba, S.-I., Pootanakit, K., & Tanapongpipat, S. (2015). Production of polyhydroxyalkanoates from crude glycerol using recombinant *Escherichia coli*. *Journal*

of Polymers and the Environment, *23*(1), 38–44. https://doi.org/10.1007/s10924-014-0681-8

Poblete-Castro, I., Binger, D., Oehlert, R., & Rohde, M. (2014). Comparison of mcl-poly(3-hydroxyalkanoates) synthesis by different *Pseudomonas putida* strains from crude glycerol: Citrate accumulates at high titer under PHA-producing conditions. *BMC Biotechnology*, *14*(1), 962. https://doi.org/10.1186/s12896-014-0110-z

Pokrovskaya, I. D., Szwedo, J. W., Goodwin, A., Lupashina, T. V., Nagarajan, U. M., & Lupashin, V. V. (2012). *Chlamydia trachomatis* hijacks intra-Golgi COG complex-dependent vesicle trafficking pathway. *Cellular Microbiology*, *14*(5), 656–668. https://doi.org/10.1111/j.1462-5822.2012.01747.x

Ravintheran, S. K., Sivaprakasam, S., Loke, S., Lee, S. Y., Manickam, R., Yahya, A., Croft, L., Millard, A., Parimannan, S., & Rajandas, H. (2019). Complete genome sequence of *Sphingomonas paucimobilis* AIMST S2, a xenobiotic-degrading bacterium. *Scientific Data*, *6*(1), 1–6. https://doi.org/10.1038/s41597-019-0289-x

Raza, Z. A., Abid, S., & Banat, I. M. (2018). Polyhydroxyalkanoates: Characteristics, production, recent developments and applications. *International Biodeterioration & Biodegradation*, *126*, 45–56. https://doi.org/10.1016/j.ibiod.2017.10.001

Rivas, A. J., Lemos, M. L., & Osorio, C. R. (2013). *Photobacterium damselae* subsp. *damselae*, a bacterium pathogenic for marine animals and humans. *Frontiers in Microbiology*, *4*(283), 1–6. https://doi.org/10.3389/fmicb.2013.00283

Rodríguez-Contreras, A., Koller, M., Miranda-de Sousa Dias, M., Calafell-Monfort, M., Braunegg, G., & Marqués-Calvo, M. S. (2015). Influence of glycerol on poly(3-hydroxybutyrate) production by *Cupriavidus necator* and *Burkholderia sacchari*. *Biochemical Engineering Journal*, *94*, 50–57. https://doi.org/10.1016/j.bej.2014.11.007

Romalde, J. L. (2002). *Photobacterium damselae* subsp. piscicida: An integrated view of a bacterial fish pathogen. *International Microbiology*, *5*(1), 3–9. https://doi.org/10.1007/s10123-002-0051-6

Ruan, J., & Li, H. (2019). Fast and accurate long-read assembly with wtdbg2. *Nature Methods*, *17*, 155–158. https://doi.org/10.1038/s41592-019-0669-3

Saitou, N., & Nei, M. (1987). The neighbor-joining method: A new method for reconstructing phylogenetic trees'. *Molecular Biology and Evolution*, *4*(4), 406–425.

Sangkharak, K., Khaithongkaeo, P., Chuaikhunupakarn, T., Choonut, A., & Prasertsan, P. (2020). The production of polyhydroxyalkanoate from waste cooking oil and its application in biofuel production. *Biomass Conversion and Biorefinery*, 1–14. https://doi.org/10.1007/s13399-020-00657-6

Sathiyanarayanan, G., Saibaba, G., Kiran, G. S., Yang, Y.-H.-H., & Selvin, J. (2017). Marine sponge-associated bacteria as a potential source for polyhydroxyalkanoates. *Critical Reviews in Microbiology*, *43*(3), 294–312. https://doi.org/10.1080/1040841X.2016.1206060

Schöner, T. A., Gassel, S., Osawa, A., Tobias, N. J., Okuno, Y., Sakakibara, Y., Shindo, K., Sandmann, G., & Bode, H. B. (2016). Aryl polyenes, a highly abundant class of bacterial natural products, are functionally related to antioxidative carotenoids. *ChemBioChem*, *17*(3), 247–253. https://doi.org/10.1002/cbic.201500474

Sedlacek, P., Slaninova, E., Koller, M., Nebesarova, J., Marova, I., Krzyzanek, V., & Obruca, S. (2019). PHA granules help bacterial cells to preserve cell integrity when exposed to sudden osmotic imbalances. *New Biotechnology*, *49*, 129–136. https://doi.org/10.1016/j.nbt.2018.10.005

Seemann, T. (2017). *ABRicate, mass screening of contigs for antimicrobial resistance or virulence genes*. Github.

Seppey, M., Manni, M., & Zdobnov, E. M. (2019). BUSCO: Assessing genome assembly and annotation completeness. *Methods in Molecular Biology*, *1962*, 227–245. https://doi.org/10.1007/978-1-4939-9173-0_14

Slaninova, E., Sedlacek, P., Mravec, F., Mullerova, L., Samek, O., Koller, M., Hesko, O., Kucera, D., Marova, I., & Obruca, S. (2018). Light scattering on PHA granules protects bacterial cells against the harmful effects of UV radiation. *Applied Microbiology and Biotechnology*, *102*(4), 1923–1931. https://doi.org/10.1007/s00253-018-8760-8

Srividhya, K. V., Alaguraj, V., Poornima, G., Kumar, D., Singh, G. P., Raghavenderan, L., Katta, A. V. S. K. M., Mehta, P., & Krishnaswamy, S. (2007). Identification of prophages in bacterial genomes by dinucleotide relative abundance difference. *PLoS One*, *2*(11), e1193. https://doi.org/10.1371/journal.pone.0001193

Stothard, P., & Wishart, D. S. (2005). Circular genome visualization and exploration using CGView. *Bioinformatics*, *21*(4), 537–539. https://doi.org/10.1093/bioinformatics/bti054

Sun, C., Pérez-Rivero, C., Webb, C., & Theodoropoulos, C. (2020). Dynamic metabolic analysis of *Cupriavidus necator* DSM545 producing poly(3-hydroxybutyric acid) from glycerol. *Processes*, *8*(6), 657. https://doi.org/10.3390/PR8060657

Tanadchangsaeng, N., & Yu, J. (2012). Microbial synthesis of polyhydroxybutyrate from glycerol: Gluconeogenesis, molecular weight and material properties of biopolyester. *Biotechnology and Bioengineering*, *109*(11), 2808–2818. https://doi.org/10.1002/bit.24546

Teufel, R., Mascaraque, V., Ismail, W., Voss, M., Perera, J., Eisenreich, W., Haehnel, W., & Fuchs, G. (2010). Bacterial phenylalanine and phenylacetate catabolic pathway revealed. *Proceedings of the National Academy of Sciences of the United States of America*, *107*(32), 14390–14395. https://doi.org/10.1073/pnas.1005399107

The Uniprot Consortium. (2019). UniProt: A worldwide hub of protein knowledge. *Nucleic Acids Research*, *47*(D1), D506–D515. https://doi.org/10.1093/nar/gky1049

Urbanczyk, H., Ast, J. C., & Dunlap, P. V. (2011). Phylogeny, genomics, and symbiosis of *Photobacterium*. *FEMS Microbiology Reviews*, *35*(2), 324–342. https://doi.org/10.1111/j.1574-6976.2010.00250.x

van Sebille, E., Wilcox, C., Lebreton, L., Maximenko, N., Hardesty, B. D., van Franeker, J. A., Eriksen, M., Siegel, D., Galgani, F., & Law, K. L. (2015). A global inventory of small floating plastic debris. *Environmental Research Letters*, *10*(12), 124006. https://doi.org/10.1088/1748-9326/10/12/124006

Van Thuoc, D., My, D. N., Loan, T. T., & Sudesh, K. (2019). Utilization of waste fish oil and glycerol as carbon sources for polyhydroxyalkanoate production by *Salinivibrio* sp. M318. *International Journal of Biological Macromolecules*, *141*, 885–892. https://doi.org/10.1016/j.ijbiomac.2019.09.063

Vastano, M., Corrado, I., Sannia, G., Solaiman, D. K. Y., & Pezzella, C. (2019). Conversion of no/low value waste frying oils into biodiesel and polyhydroxyalkanoates. *Scientific Reports*, *9*(1), 1–8. https://doi.org/10.1038/s41598-019-50278-x

Vázquez-Rosas-Landa, M., Ponce-Soto, G. Y., Eguiarte, L. E., & Souza, V. (2017). Comparative genomics of free-living *Gammaproteobacteria*: pathogenesis-related genes or interaction-related genes? *Pathogens and Disease*, *75*(5), 1–12. https://doi.org/10.1093/FEMSPD/FTX059

Vesth, T., Wassenaar, T. M., Hallin, P. F., Snipen, L., Lagesen, K., & Ussery, D. W. (2010). On the origins of a *Vibrio* species. *Microbial Ecology*, *59*(1), 1–13. https://doi.org/10.1007/s00248-009-9596-7

Wang, Y., Yin, J., & Chen, G.-Q. (2014). Polyhydroxyalkanoates, challenges and opportunities. *Current Opinion in Biotechnology*, *30C*, 59–65. https://doi.org/10.1016/j.copbio.2014.06.001

Watson, M., & Warr, A. (2019). Errors in long-read assemblies can critically affect protein prediction. *Nature Biotechnology*, *37*(2), 124–126. https://doi.org/10.1038/s41587-018-0004-z

Wick, R. R., Schultz, M. B., Zobel, J., & Holt, K. E. (2015). Bandage: Interactive visualization of *de novo* genome assemblies: Figure 1. *Bioinformatics*, *31*(20), 3350–3352. https://doi.org/10.1093/bioinformatics/btv383

Xiao, N., & Jiao, N. (2011). Formation of polyhydroxyalkanoate in aerobic anoxygenic phototrophic bacteria and its relationship to carbon source and light availability. *Applied and Environmental Microbiology, 77*(21), 7445–7450. https://doi.org/10.1128/AEM.05955-11

Yoon, S.-H., Ha, S.-M., Kwon, S., Lim, J., Kim, Y., Seo, H., & Chun, J. (2017). Introducing EzBioCloud: A taxonomically united database of 16S rRNA gene sequences and whole-genome assemblies. *International Journal of Systematic and Evolutionary Microbiology, 67*(5), 1613–1617. https://doi.org/10.1099/ijsem.0.001755

Zankari, E., Hasman, H., Cosentino, S., Vestergaard, M., Rasmussen, S., Lund, O., Aarestrup, F. M., & Larsen, M. V. (2012). Identification of acquired antimicrobial resistance genes. *Journal of Antimicrobial Chemotherapy, 67*(11), 2640–2644. https://doi.org/10.1093/jac/dks261

Zhang, J., Shishatskaya, E. I., Volova, T. G., da Silva, L. F., & Chen, G.-Q. (2018). Polyhydroxyalkanoates ({PHA}) for therapeutic applications. *Materials Science and Engineering: C, 86*, 144–150. https://doi.org/10.1016/j.msec.2017.12.035
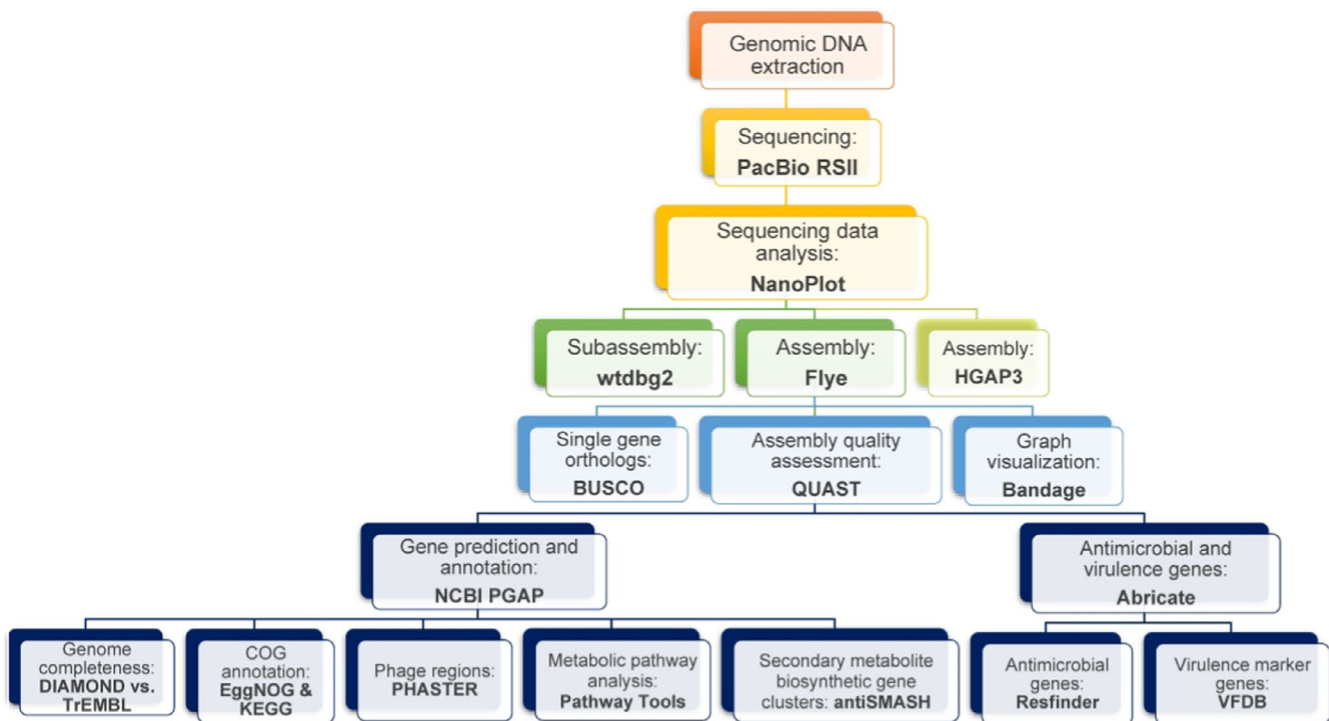
APPENDIX

Figure A1   Flow diagram showing the overview of the study design

TABLE A1 General features of *P. ganghwense* strain C2.2 based on MIGS mandatory information

Items	Description
Submitted to INSDC	SRA, BioProject, Genome
Investigation type	Bacteria
Project name	Complete genome sequence of *Photobacterium ganghwense* C2.2
Geographic location	44.215993, 29.656308
Geographic location name	Romania, Constanta, Black Sea
Collection date	2/15/2018
Environment (biome)	Shore
Environment (feature)	Seashore
Environment (material)	Sea sand
Environmental package	Sediment
Subspecific genetic lineage	Strain C2.2
Number of replicons	2
Extrachromosomal elements	1
Estimated size	5,744,420 bp
Observed biotic relationship	Free-living
Trophic level	Heterotroph
Relationship to oxygen	Aerobic
Sequencing method	PacBio RSII
Finishing strategy (status; coverage; contigs)	Complete; 113; 3
Sediment depth	0 m
Sediment elevation	0 m
Sediment particle classification	Sand
Sediment pH	7
Sediment salinity	17‰
Sediment temperature	2°C

TABLE A2 BUSCO evaluation of the completeness of *P. ganghwense* C2.2 genome assemblies

BUSCO	*Bacteria* BUSCOs		*Vibrionales* BUSCOs	
	HGAP3	Flye	HGAP3	Flye
Complete BUSCOs	99.2% (123)	100% (124)	98.2% (1420)	99.6% (1439)
Complete and single-copy BUSCOs	98.4% (122)	99.2% (123)	97.9% (1425)	99.3% (1435)
Complete and duplicated BUSCOs	0.8% (1)	0.8% (1)	0.3% (5)	0.3% (4)
Fragmented BUSCOs	0% (0)	0% (0)	0.7% (10)	0.1% (2)
Missing BUSCOs	0.8% (1)	0% (0)	1.1% (15)	0.3% (5)
Total BUSCO groups searched	124	1445		

Program	Version	Specific parameters used
NanoPlot	1.28.2	--plots hex dot
wtdbg2	2.5	-A -c rs -g 5.8m -S 2
Flye	2.6	--pacbio-raw [subreads.fastq] --subassemblies [wtdbg2.fasta] --genome-size 5.8m -i 2
Bandage	0.8.1	
seqtk	1.3-r106	seq -r
Quast	5.0.2	-f --pacbio
BUSCO	4.0.1	--auto-lineage-prok -m geno --long
DIAMOND	0.9.29.130	--db [TrEMBL db] -f 6 --max-target-seqs 1
EggNOG Mapper	2.0.1	-m diamond
Abricate	0.5	--db [vfdb/resfinder]
Pathway Tools	23.5	
antiSMASH	5.1.2	
Database	**Version**	
VFDB	2020 -01-17	
Resfinder	2019-10-01	
TrEMBL	2019-12-11	
EggNOG	5.0.0	

TABLE A3 The bioinformatics tools, software versions, specific settings, and databases used in this study